

## Real-time CT testing of rock damage evolution mechanism under triaxial compression

Xiurun Ge

Key Laboratory of Rock and Soil Mechanics, Institute of Rock and Soil Mechanics, CAS, Wuhan, Hubei, China  
Institute of Geotechnical Mechanics and Engineering, Shanghai Jiaotong University, Shanghai, China

Jianxi Ren

School of Architecture and Civil Engineering, Xi'an University of Science and Technology, Xi'an, Shaanxi, China

**ABSTRACT:** In this paper, specified triaxial loading equipment corresponding to the X-ray computerized tomography (CT) machine has been developed. It can be used to accomplish meso-damage evolution CT real in time testing of rock, soil, frozen rock, frozen soil and ice under triaxial compression loading, unloading, fatigue and creep stress state. The real-time CT testing of the meso-damage propagation law of the whole sandstone failure process under triaxial compression has been completed using the above equipment. Through the CT scanning, the clear CT images, which include from the microcracks compressed stage to growth stage, bifurcation stage, development stage, crack fracture stage, the rock sample failure until to unloading stage in the different stress states were obtained. The CT values, CT images and the other data have been analyzed. Based on the results of the CT testing of meso-damage evolution law of rock, the stress threshold value of meso-damage of rock is given, and the stress-strain complete process curve of rock is divided into 5 segments. The initial rock damage propagation law is given in this paper.

### 1 INTRODUCTION

The study of rock damage mechanics is, at present, one of the important topics in rock mechanics (Dragon and Mroz, 1979). Meso-testing provides an experimental basis for macro-damage theory and helps in the understanding of the rock damage mechanism when using either the scanned electronic microscope or the optical microscope; the computerized tomography (CT) technique has many advantages in non-destructive scanning, designation of multiple planes, and introduction of international standard specimens.

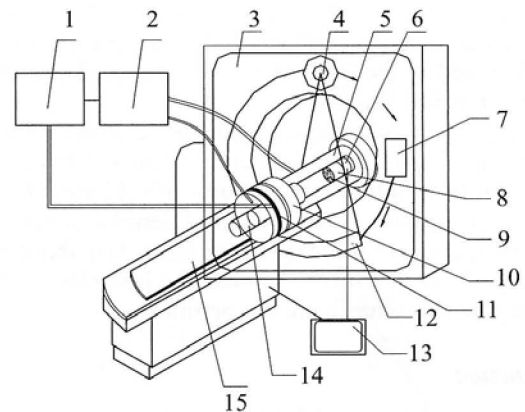
Yang et al. (1998) and Kawakata et al. (1997) conducted studies on the initial meso-damage properties of rocks by using CT scanning and discussed the characters of damage propagation. It should be noted that the experimental studies were performed on specimens that were pre-damaged by using a MTS testing machine. Obviously, such a CT scanning procedure is not carried out under real-time and the unloading procedure used has considerable effects on CT examination results.

It is the purpose of the present technical note to develop a real-time CT scanning equipment to be used for studying the damage evolution law of rocks during triaxial compression tests. No reports have been published on the subject so far and the testing method described is to be considered highly innovative in rock mechanics.

### 2 SPECIAL TRIAXIAL LOADING EQUIPMENT

#### 2.1 Principle

The main parts of CT testing system consist of cold bathing control sub-system, displacement and loading control sub-system, triaxial chamber and image processing sub-system (Figure 1). It allows one to perform a real-time examination



1. cold bathing control sub-system 2. displacement and loading control sub-system 3. scan frame of CT machine 4. X-ray source 5. sample installing tank 6. loading sensor 7. CT mold/data convertor 8. sample 9. scan section 10. pressure head 11. triaxial chamber 12. detector 13. image processing sub-system 14. displacement sensor 15. testing platform

Figure 1. Principle of special triaxial loading testing equipment.

of rock or soil specimens subjected to triaxial compression in normal or below-zero temperature environments. A tomograph is employed to perform a multi-plane damage examination by CT images of a given special cross-section at different stress levels. A real 3-D image is made to describe the damage configuration of a rock specimen by using a rebuilding technique of images. The cylinders used for testing are 50 mm in diameter and 100 mm in length.

The triaxial testing chamber is 240 mm in diameter and 1000 mm in height. It was designed for 400 kN axial compression load and a 20 MPa confining pressure. The chamber is placed in the scanning area of the tomograph in order to reduce the effect of chamber material on the scanning results.

Table 1. Kinds of CT testing of special triaxial loading testing equipment.

Media	Rock, soil, frozen rock, frozen soil, ice
Temperature	Normal atmospheric temperature, negative temperature
Loading method	Successive compression loading, unloading, fatigue loading, creep loading
Confining pressure	Triaxial, uniaxial

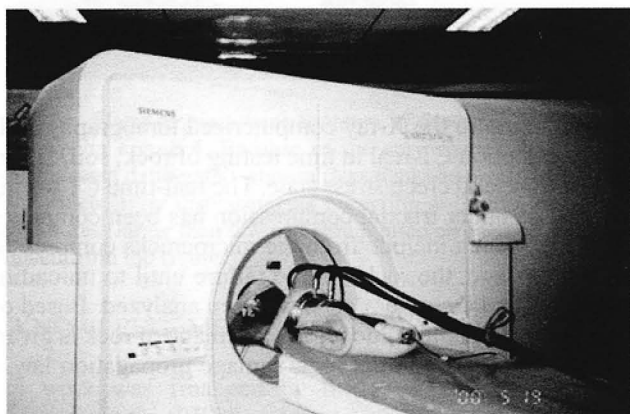


Figure 2. Photo of real-time CT testing scene.

It is made of top-quality light metal of LY12—a kind of carbide for aeroplane manufacture. The triaxial testing chamber is designed by the CT unit of the State Key Laboratory of China Frozen Soil Engineering.

A X-ray spiral tomograph of SIEMENS SOMATOM plus type, having a spatial resolution of  $0.35 \text{ mm} \times 0.35 \text{ mm}$ , capable of identifying a minimum volume of  $0.12 \text{ mm}^3$  (1 mm in layer thickness) with the resolution of density contrast being 0.3%(3Hu), is used for the CT equipment. The above resolution meets the requirement of lower size limit ( $10^{-4} \text{ m}$ ) that is necessary for meso mechanics experiments.

## 2.2 Function

The above special triaxial loading testing equipment can be used to accomplished many kinds of CT testing (Table 1).

## 2.3 Testing method

The testing chamber is placed horizontally on a bed and the rock specimen is positioned within the scanning limits of the CT unit (Figure 2). The difference section can be scanned in difference stress-strain state in the processing of loading of sample. The change law of CT images and CT number of sample can be researched.

It is advisable to carry out a series of tests in a stiff testing machine before performing the meso CT tests, given the cost of CT examination.

Comparing to the CT testing in normal atmospheric temperature, the difference point of CT testing in negative temperature is that it is needed negative temperature condition by the cold bathing control sub-system.

## 2.4 Testing results

Using the above equipment, the large CT real-time testing of meso-damage evolution of rock, soil, frozen rock, frozen soil

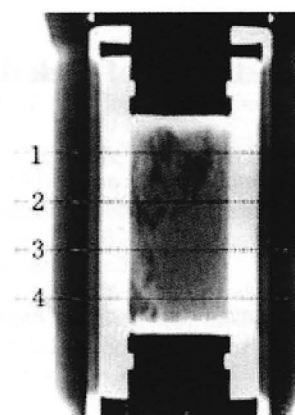


Figure 3. Scan section position with the rock sample.

and ice have been accomplished (Ge et al, 2004). The damage variable based on CT number is given. The concept of CT number reduction rate is defined. The estimate formula of width of CT crack is given. The equation of rock damage evolution and constitutive is created (Ge et al, 1999, 2004). The results of the meso-damage propagation mechanism of sandstone under triaxial loading compression will be showed in the following fragment.

## 3 REAL-TIME EXPERIMENTS OF ROCK DAMAGE PROPAGATION

### 3.1 Procedure and method

In order to increase reliability and allow for appropriate comparison of data, all the specimens to be tested should be as far as possible homogeneous in nature. For this reason, both sampling and specimen preparation need to be performed in strictly controlled conditions by overcoving from a large size rock block and by avoiding any possible disturbance.

The sandstone blocks used in this work were sampled from the Nanqiao Coal Mine of Pubai Mining Bureau, Shan'xi Province. The real-time CT scanning experiments were performed on sandstone specimens under triaxial compression testing conditions. Four tomographic planes were selected for each specimen, as shown in Figure 3, where numbers 1, 2, 3 and 4 indicate these planes. During loading, the real-time CT scanning was performed on the tomographic planes for various loading levels; the variation in image during the complete loading process (fracture initiation, branching development and failure) of each tomographic plane has been carefully observed, in order study the damage mechanism from the point of meso scale.

### 3.2 Interpretation of testing results

Taking as an example the sandstone specimen No. 5, the results obtained with be illustrated in the following. The test was carried out in closely controlled conditions with a static rate of  $2.75 \times 10^{-5} \text{ /s}$  and 55 minutes duration. The fifth generation of spiral CT unit was employed for testing. This tomograph has a stronger parallel processing capacity, so that the scanning on a certain tomographic plane starts when the scanning on the previous plane has not been completed. Accordingly, the scanning of all the four cross-sections can be performed almost simultaneously within a short time. If the old CT unit had been used, the scanning work would have required a couple of minutes; in

Table 2. Stress state corresponding to each scanning on specimen No.5 ( $\sigma_2 = \sigma_3 = 10$  MPa).

Sequence of scanning	$\sigma_1$ /MPa	$\sigma_1 - \sigma_3$ /MPa	$\epsilon_1$ /‰	Remarks
1	11.88	1.88	0.63	
2	22.63	12.63	2.5	
3	35.92	25.92	5.0	Threshold value
4	45.66	35.66	6.9	
5	48.85	38.85	7.6	
6	49.47	39.47	7.9	
7	51.71	41.71	8.5	
8	40.79	30.79	11.6	Unloading

Note:  $\sigma_1$ : axial stress,  $\sigma_2, \sigma_3$ : confining pressure,  $\epsilon_1$ : axial strain.

Table 3. Testing results (1).

Sequence of scanning	1st scan section CT number/variance	2nd scan section CT number/variance
1	1625.6/98.95	1630.0/102.07
2	1626.6/104.52	1633.6/104.51
3	1627.6/105.50	1634.3/104.74
4	1626.6/105.63	1634.2/102.19
5	1625.9/104.35	1632.0/101.07
6	1624.5/101.54	1627.4/100.71
7	1622.9/97.53	1621.5/99.87
8	1609.9/91.56	1604.3/113.37

Table 4. Testing results (2).

Sequence of scanning	3rd scan section CT number/variance	4th scan section CT number/variance
1	1592.6/105.01	1582.3/172.03
2	1598.2/105.10	1583.5/172.86
3	1601.1/104.94	1584.5/166.57
4	1602.3/104.07	1585.2/166.76
5	1601.9/101.05	1584.8/166.67
6	1596.7/97.11	1581.5/165.44
7	1591.0/98.84	1578.7/165.74
8	1576.9/115.51	1565.4/183.29

other words, the continuous evolution of rock damage within this time interval would have had serious effects on both quality and realism of CT images (corresponding to a given state of stress). The stress conditions corresponding to an 8-time scanning sequence on sandstone specimen No.5 are shown in Table 2. The CT testing results can be found in Tables 3, 4. The CT images can be found in Figure 4. The complete stress-strain curve obtained during testing of the same specimen is illustrated in Figure 5, where also shown are the numbers 1 to 8 which give the scanning sequence. In the meantime, the numbers 1 to 8 which denote the scanning sequence of specimen No.5 is shown in Figure 5. Figure 6 is the change law of CT number of specimen No.5. It is observed that the stress-strain complete process curve of rock can be divided into 5 segments based on CT number change law (Figure 7).

The first stage (OA segment in Figures 6 and 7) is interpreted as damage weakening. In this stage, axial stress  $\sigma_1$  increases from 11.88 MPa to 22.63 MPa; the CT number of

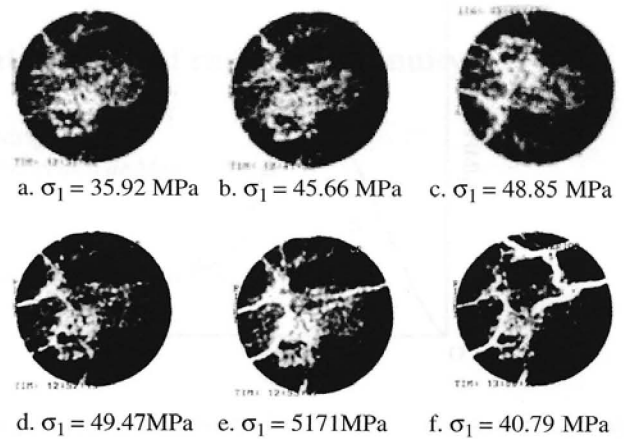


Figure 4. CT images of section 1 after threshold value.

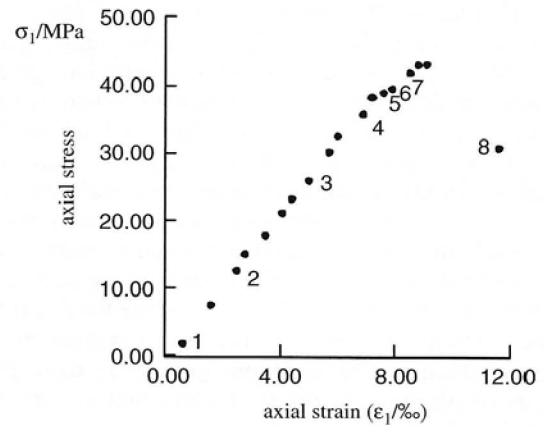


Figure 5. Stress state corresponding to each scanning condition.

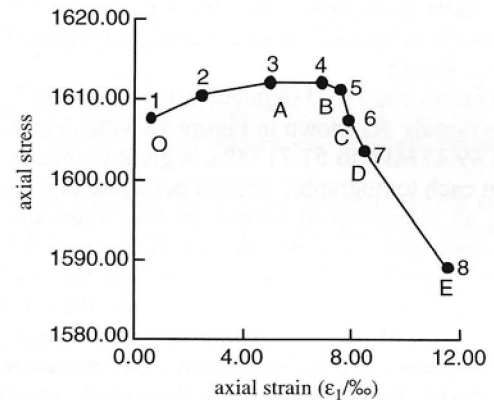


Figure 6. Relationship between scanning condition and change law of CT number.

four tomographic sections or the CT number of the rock specimens (mean value of four tomographic CT numbers) increases, initial micro-cracks and void (primary damage) close, to cause closing-up and increment of density (the image is omitted owing to limited space).

During the second stage (AB segment in Figures 6 and 7),  $\sigma_1$  increases from 22.63 MPa to 35.92 MPa. We can see that both the CT number and its variance keep nearly constant as the rock is in elastic deformation. As shown in Figure 4a, the initiation and branching of a small number of cracks appear just when  $\sigma_1 = 35.92$  MPa. It is the stress threshold values of specimen No. 5.

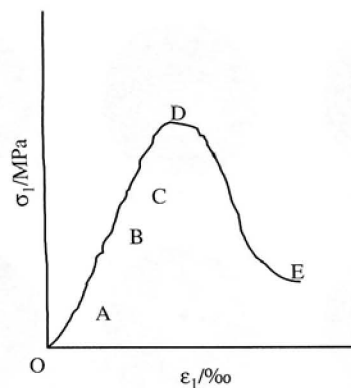


Figure 7. Segment of stress-strain whole process curve.

The third stage (BC segment in Figures 6 and 7) starts after stage 2 and ends when the threshold value increases to 49.47 MPa, i.e., it is the stress value where damage evolution starts and develops in a stable manner. When  $\sigma_1$  reaches 45.66 MPa, the CT number of the first and second tomographic sections decreases and extension and branching of original cracks take place accompanied by initiation of new cracks, as shown in Figure 4b. This is interpreted as an indication of crack initiation, as shown in the last scanning—bright points (lower density areas) arise locally on the scanned section. In the meantime, the CT number of the third and fourth scanned sections increases a little, accompanied by crack initiation, which results in inhomogeneity in damage evolution as obtained from meso experimental results. When  $\sigma_1 = 48.85$  MPa (Figure 4c), the cracks initiating in the previous stage start extending, with a number of new cracks initiating simultaneously when the CT number of all scanned sections starts to decrease. Besides, variance of CT number has somewhat increased and micro cracks initiate and develop in the rock specimen.

In the fourth stage (CD segment in Figures 6 and 7) damage develops rapidly. As shown in Figure 4e with an increment of  $\sigma_1$  from 49.47 MPa to 51.71 MPa, a great number of micro-cracks in each tomographic section penetrate into each other, showing an indication of failure. In this stage, the damage of rock specimen develops rapidly. When  $\sigma_1 = 53.12$  MPa, i.e. when the peak axial strength is reached, the cracks penetrate through the specimen completely and the CT scanning fails due to rapid decrease of stress. In this stage, the CT number decreases at a higher velocity, the increment in variance increases, the micro-cracks go through the specimen and micro joints appear, and the rock specimen quickly reaches its peak strength.

In the fifth or final stage (DE segment in Figures 6 and 7), post damage (after peak value) develops rapidly. When  $\sigma_1$  is unloaded from  $\sigma_{c1}$  (peak value) to 40.79 MPa, several major thoroughgoing joints are widened, as shown in Figure 4f. We have observed at this stage a sudden decrease in the CT number, with a variance increase up to ten times. The

resultant macro joints open rapidly and the rock specimen dilates abruptly in volume.

#### 4 DISCUSSION AND CONCLUSIONS

The specified triaxial loading equipment used to study meso-damage evolution law of geotechnical media under different loading conditions corresponding to the X-ray CT machine have been successfully developed. The measurement of real-time CT testing does provide an innovative testing method for study of the damage mechanism of rock and soil at a meso-size level. Experiments have shown that it is an advanced and feasible testing method and it will strongly enhance the development of testing techniques for damage mechanics of rock and soil. Furthermore, the development of advanced meso-testing technique provides an important experimental basis for study of macro-damage theory of rock and soil.

The above triaxial CT testing gave clear images of the micro voids development of rock material in such steps as closing-up of voids, fracture initiation, branching, development of micro-cracks, rupture, failure and unloading. The results showed that the damage evolution of rock is a non-linear dynamic process. In the fact, rock is a typical material that has been damaged originally and its damage evolution manifests itself in localization and inhomogeneity. The test results are satisfactory.

According to the results obtained from the meso-testing for rock damage evolution, the threshold value of stress damage of rock has been given and the stress-strain curve of rocks has been divided into five stages. This quantitative division is very important to the establishment of a stage-wise constitutive model and damage evolution of rocks.

#### ACKNOWLEDGEMENT

Financial support from the National Natural Science Foundation of China under grant No.10172057 and No.10202019 is gratefully acknowledged.

#### REFERENCES

- Dragon, A. & Mroz, Z. 1979. A continuum model for plastic brittle behavior of rock and concrete. *Int. J. Eng. Sci.*, 17(1): 121~137.
- Ge, X.R., Ren, J.X., Pu, Y.B., Ma, W., Zhu, Y.L., 1999. A real in time CT triaxial testing study of meso damage evolution law of coal, *Chinese Journal of Rock Mechanics and Engineering*, 18(5), 497~502.
- Ge, X.R., Ren, J.X., Pu, Y.B., Ma, W., Sun, H., 2004. *Macro and meso testing study on damage mechanics of geotechnical media*. Beijing: Science Press.
- KawaKata, H., Cho, A. T., Yanagidani, M.S., et al. 1997.: The observations of faulting in Westerly granite under triaxial compression by X-ray CT scan. *Int. Journal. Rock Mechanics and Mining Science*. 34 (3~4), 151~162.
- Yang, G.S. & Zhang, C.Q. 1998: *Rock masses damage and identification*, Xi'an: Shaanxi Science and Technology Press.